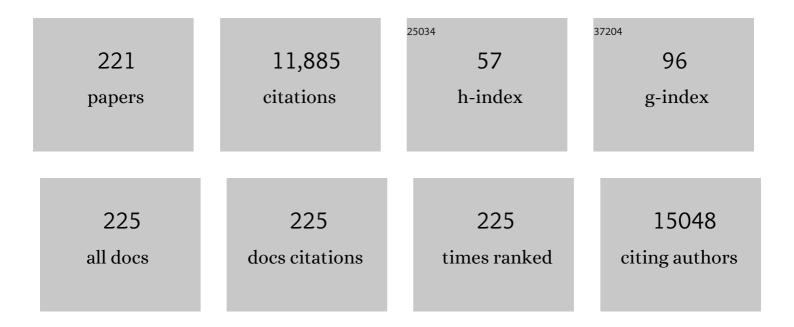
List of Publications by Year in descending order

Source: https://exaly.com/author-pdf/2110395/publications.pdf Version: 2024-02-01



Ηενοίι Ηλνι

#	Article	IF	CITATIONS
1	Graphene oxide exhibits broad-spectrum antimicrobial activity against bacterial phytopathogens and fungal conidia by intertwining and membrane perturbation. Nanoscale, 2014, 6, 1879-1889.	5.6	504
2	Facile synthesis of fluorescent carbon dots using watermelon peel as a carbon source. Materials Letters, 2012, 66, 222-224.	2.6	471
3	Antiviral Activity of Graphene Oxide: How Sharp Edged Structure and Charge Matter. ACS Applied Materials & Interfaces, 2015, 7, 21571-21579.	8.0	292
4	Nano-magnetic catalyst KF/CaO–Fe3O4 for biodiesel production. Applied Energy, 2011, 88, 2685-2690.	10.1	270
5	Preparation of KF/CaO nanocatalyst and its application in biodiesel production from Chinese tallow seed oil. Fuel, 2010, 89, 2267-2271.	6.4	244
6	Antibacterial Activity of Graphene Oxide/g-C <sub>3</sub> N <sub>4</sub> Composite through Photocatalytic Disinfection under Visible Light. ACS Sustainable Chemistry and Engineering, 2017, 5, 8693-8701.	6.7	224
7	Gecko-Inspired Nanotentacle Surface-Enhanced Raman Spectroscopy Substrate for Sampling and Reliable Detection of Pesticide Residues in Fruits and Vegetables. Analytical Chemistry, 2017, 89, 2424-2431.	6.5	216
8	Cauliflower-Inspired 3D SERS Substrate for Multiple Mycotoxins Detection. Analytical Chemistry, 2019, 91, 3885-3892.	6.5	200
9	Probing the Interaction of Magnetic Iron Oxide Nanoparticles with Bovine Serum Albumin by Spectroscopic Techniques. Journal of Physical Chemistry B, 2009, 113, 10454-10458.	2.6	197
10	Multi-walled carbon nanotubes can enhance root elongation of wheat (Triticum aestivum) plants. Journal of Nanoparticle Research, 2012, 14, 1.	1.9	175
11	Multisite Inhibitors for Enteric Coronavirus: Antiviral Cationic Carbon Dots Based on Curcumin. ACS Applied Nano Materials, 2018, 1, 5451-5459.	5.0	165
12	Facile synthesis of melamine-based porous polymer networks and their application for removal of aqueous mercury ions. Polymer, 2010, 51, 6193-6202.	3.8	159
13	Utilization of waste freshwater mussel shell as an economic catalyst for biodiesel production. Biomass and Bioenergy, 2011, 35, 3627-3635.	5.7	155
14	Synthesis of nitrogen-doped porous graphitic carbons using nano-CaCO3 as template, graphitization catalyst, and activating agent. Carbon, 2012, 50, 3753-3765.	10.3	151
15	Evaluation and mechanism of antifungal effects of carbon nanomaterials in controlling plant fungal pathogen. Carbon, 2014, 68, 798-806.	10.3	141
16	Glutathione-Capped Ag <sub>2</sub> S Nanoclusters Inhibit Coronavirus Proliferation through Blockage of Viral RNA Synthesis and Budding. ACS Applied Materials & Interfaces, 2018, 10, 4369-4378.	8.0	141
17	From Electrochemistry to Electroluminescence: Development and Application in a Ratiometric Aptasensor for Aflatoxin B1. Analytical Chemistry, 2017, 89, 7578-7585.	6.5	139
18	pHâ€Responsive, Lightâ€Triggered onâ€Demand Antibiotic Release from Functional Metal–Organic Framework for Bacterial Infection Combination Therapy. Advanced Functional Materials, 2018, 28, 1800011.	14.9	137

#	Article	IF	CITATIONS
19	Quantum Dot-Based Near-Infrared Electrochemiluminescent Immunosensor with Gold Nanoparticle-Graphene Nanosheet Hybrids and Silica Nanospheres Double-Assisted Signal Amplification. Analytical Chemistry, 2012, 84, 4893-4899.	6.5	129
20	Ultrasensitive detection of aflatoxin B 1 by SERS aptasensor based on exonuclease-assisted recycling amplification. Biosensors and Bioelectronics, 2017, 97, 59-64.	10.1	128
21	Graphene Oxide-Silver Nanocomposite: Novel Agricultural Antifungal Agent against <i>Fusarium graminearum</i> for Crop Disease Prevention. ACS Applied Materials & Interfaces, 2016, 8, 24057-24070.	8.0	126
22	Acidityâ€Triggered Tumorâ€Targeted Chimeric Peptide for Enhanced Intraâ€Nuclear Photodynamic Therapy. Advanced Functional Materials, 2016, 26, 4351-4361.	14.9	122
23	Carbon dots as inhibitors of virus by activation of type I interferon response. Carbon, 2016, 110, 278-285.	10.3	121
24	A new function of graphene oxide emerges: inactivating phytopathogenic bacterium Xanthomonas oryzae pv. Oryzae. Journal of Nanoparticle Research, 2013, 15, 1.	1.9	120
25	Aqueous synthesis of porous platinum nanotubes at room temperature and their intrinsic peroxidase-like activity. Chemical Communications, 2013, 49, 6024.	4.1	114
26	Virus Capture and Destruction by Labelâ€Free Graphene Oxide for Detection and Disinfection Applications. Small, 2015, 11, 1171-1176.	10.0	113
27	Biocompatible and Highly Luminescent Near-Infrared CuInS <sub>2</sub> /ZnS Quantum Dots Embedded Silica Beads for Cancer Cell Imaging. ACS Applied Materials & Interfaces, 2014, 6, 2011-2017.	8.0	109
28	Tumor-Triggered Geometrical Shape Switch of Chimeric Peptide for Enhanced <i>in Vivo</i> Tumor Internalization and Photodynamic Therapy. ACS Nano, 2017, 11, 3178-3188.	14.6	109
29	Carbon-Dot and Quantum-Dot-Coated Dual-Emission Core–Satellite Silica Nanoparticles for Ratiometric Intracellular Cu <sup>2+</sup> Imaging. Analytical Chemistry, 2016, 88, 7395-7403.	6.5	108
30	Endogenous stimulus-powered antibiotic release from nanoreactors for a combination therapy of bacterial infections. Nature Communications, 2019, 10, 4464.	12.8	108
31	A novel method for the determination of Pb2+ based on the quenching of the fluorescence of CdTe quantum dots. Mikrochimica Acta, 2008, 161, 81-86.	5.0	107
32	Study on the interaction between bovine serum albumin and CdTe quantum dots with spectroscopic techniques. Journal of Molecular Structure, 2008, 892, 116-120.	3.6	107
33	Synergistic antibacterial effects of curcumin modified silver nanoparticles through ROS-mediated pathways. Materials Science and Engineering C, 2019, 99, 255-263.	7.3	107
34	Hierarchical Nanogaps within Bioscaffold Arrays as a High-Performance SERS Substrate for Animal Virus Biosensing. ACS Applied Materials & Interfaces, 2014, 6, 6281-6289.	8.0	105
35	Target-triggered signal-on ratiometric electrochemiluminescence sensing of PSA based on MOF/Au/G-quadruplex. Biosensors and Bioelectronics, 2018, 118, 160-166.	10.1	103
36	Atomic Vacancies Control of Pdâ€Based Catalysts for Enhanced Electrochemical Performance. Advanced Materials, 2018, 30, 1704171.	21.0	102

#	Article	IF	CITATIONS
37	A fast and sensitive immunoassay of avian influenza virus based on label-free quantum dot probe and lateral flow test strip. Talanta, 2012, 100, 1-6.	5.5	101
38	Evaluation of antibacterial effects of carbon nanomaterials against copper-resistant Ralstonia solanacearum. Colloids and Surfaces B: Biointerfaces, 2013, 103, 136-142.	5.0	101
39	Metal-organic frameworks-based sensitive electrochemiluminescence biosensing. Biosensors and Bioelectronics, 2020, 164, 112332.	10.1	99
40	Antiviral Activity of Graphene Oxide–Silver Nanocomposites by Preventing Viral Entry and Activation of the Antiviral Innate Immune Response. ACS Applied Bio Materials, 2018, 1, 1286-1293.	4.6	94
41	Interaction between fluorescein isothiocyanate and carbon dots: Inner filter effect and fluorescence resonance energy transfer. Spectrochimica Acta - Part A: Molecular and Biomolecular Spectroscopy, 2017, 171, 311-316.	3.9	87
42	Microbial synthesis of highly dispersed PdAu alloy for enhanced electrocatalysis. Science Advances, 2016, 2, e1600858.	10.3	85
43	Aqueous one-pot synthesis of bright and ultrasmall CdTe/CdS near-infrared-emitting quantum dots and their application for tumor targeting in vivo. Chemical Communications, 2012, 48, 4971.	4.1	84
44	Electrochemiluminecence nanogears aptasensor based on MIL-53(Fe)@CdS for multiplexed detection of kanamycin and neomycin. Biosensors and Bioelectronics, 2019, 129, 100-106.	10.1	83
45	Electrogenerated chemiluminescence from thiol-capped CdTe quantum dots and its sensing application in aqueous solution. Analytica Chimica Acta, 2007, 596, 73-78.	5.4	81
46	Size-dependent electrochemiluminescence behavior of water-soluble CdTe quantum dots and selective sensing of l-cysteine. Talanta, 2009, 77, 1654-1659.	5.5	75
47	Application of Multiplexed Aptasensors in Food Contaminants Detection. ACS Sensors, 2020, 5, 3721-3738.	7.8	75
48	Design of Gold Hollow Nanorods with Controllable Aspect Ratio for Multimodal Imaging and Combined Chemo-Photothermal Therapy in the Second Near-Infrared Window. ACS Applied Materials & Interfaces, 2018, 10, 36703-36710.	8.0	74
49	Targeted Near-Infrared Fluorescent Turn-on Nanoprobe for Activatable Imaging and Effective Phototherapy of Cancer Cells. ACS Applied Materials & Interfaces, 2016, 8, 15013-15023.	8.0	69
50	Surface-imprinted SiO2@Ag nanoparticles for the selective detection of BPA using surface enhanced Raman scattering. Sensors and Actuators B: Chemical, 2018, 258, 566-573.	7.8	69
51	Quantumâ€dotsâ€based fluoroimmunoassay for the rapid and sensitive detection of avian influenza virus subtype H5N1. Luminescence, 2010, 25, 419-423.	2.9	68
52	Bioapplications of DNA nanotechnology at the solid–liquid interface. Chemical Society Reviews, 2019, 48, 4892-4920.	38.1	68
53	One-step growth of high luminescence CdTe quantum dots with low cytotoxicity in ambient atmospheric conditions. Dalton Transactions, 2010, 39, 7017.	3.3	67
54	Signal-Amplified Near-Infrared Ratiometric Electrochemiluminescence Aptasensor Based on Multiple Quenching and Enhancement Effect of Graphene/Gold Nanorods/G-Quadruplex. Analytical Chemistry, 2016, 88, 8179-8187.	6.5	67

#	Article	IF	CITATIONS
55	Precisely Striking Tumors without Adjacent Normal Tissue Damage <i>via</i> Mitochondria-Templated Accumulation. ACS Nano, 2018, 12, 6252-6262.	14.6	65
56	Mitochondria-Targeted Chimeric Peptide for Trinitarian Overcoming of Drug Resistance. ACS Applied Materials & Interfaces, 2016, 8, 25060-25068.	8.0	61
57	Sensitive detection of melamine by an electrochemiluminescence sensor based on tris(bipyridine)ruthenium(II)-functionalized metal-organic frameworks. Sensors and Actuators B: Chemical, 2018, 265, 378-386.	7.8	60
58	A novel method for the preparation of water-soluble and small-size CdSe quantum dots. Materials Letters, 2006, 60, 3782-3785.	2.6	59
59	Hydrothermal synthesis of high-quality type-II CdTe/CdSe quantum dots with near-infrared fluorescence. Journal of Colloid and Interface Science, 2010, 351, 83-87.	9.4	58
60	Nitrogen-Doped Carbon Quantum Dots for Preventing Biofilm Formation and Eradicating Drug-Resistant Bacteria Infection. ACS Biomaterials Science and Engineering, 2019, 5, 4739-4749.	5.2	58
61	Photothermally triggered nitric oxide nanogenerator targeting type IV pili for precise therapy of bacterial infections. Biomaterials, 2021, 268, 120588.	11.4	57
62	Miniature Hollow Gold Nanorods with Enhanced Effect for In Vivo Photoacoustic Imaging in the NIRâ€∦ Window. Small, 2020, 16, e2002748.	10.0	56
63	Programmable DNA Tweezer-Actuated SERS Probe for the Sensitive Detection of AFB <sub>1</sub> . Analytical Chemistry, 2020, 92, 4900-4907.	6.5	56
64	Enhanced electrochemiluminescence of CdTe quantum dots with carbon nanotube film and its sensing of methimazole. Electrochimica Acta, 2009, 54, 1389-1394.	5.2	55
65	One Stone with Two Birds: Functional Gold Nanostar for Targeted Combination Therapy of Drug-Resistant <i>Staphylococcus aureus</i> Infection. ACS Applied Materials & Interfaces, 2019, 11, 32659-32669.	8.0	54
66	Electrogenerated chemiluminescence of blue emitting ZnSe quantum dots and its biosensing for hydrogen peroxide. Biosensors and Bioelectronics, 2010, 25, 1843-1846.	10.1	53
67	Synthesis of functionalized 3D porous graphene using both ionic liquid and SiO <sub>2</sub> spheres as "spacers―for high-performance application in supercapacitors. Nanoscale, 2015, 7, 659-669.	5.6	53
68	Ultrasensitive SERS detection of Bacillus thuringiensis special gene based on Au@Ag NRs and magnetic beads. Biosensors and Bioelectronics, 2017, 92, 321-327.	10.1	53
69	Study on DNA damage induced by CdSe quantum dots using nucleic acid molecular "light switches―as probe. Talanta, 2007, 71, 1675-1678.	5.5	52
70	Enzymatic biosensor of horseradish peroxidase immobilized on Au-Pt nanotube/Au-graphene for the simultaneous determination of antioxidants. Analytica Chimica Acta, 2016, 933, 89-96.	5.4	52
71	Functional peptide-based nanoparticles for photodynamic therapy. Journal of Materials Chemistry B, 2018, 6, 25-38.	5.8	52
72	A novel strategy for selective detection of Ag+ based on the red-shift of emission wavelength of quantum dots. Mikrochimica Acta, 2009, 167, 281-287.	5.0	51

HEYOU HAN

#	Article	IF	CITATIONS
73	Enzyme induced molecularly imprinted polymer on SERS substrate for ultrasensitive detection of patulin. Analytica Chimica Acta, 2020, 1101, 111-119.	5.4	51
74	Electrochemiluminescence aptasensor for multiple determination of Hg2+ and Pb2+ ions by using the MIL-53(Al)@CdTe-PEI modified electrode. Analytica Chimica Acta, 2020, 1100, 232-239.	5.4	51
75	Preparation of Mesoporous Nanosized KF/CaO–MgO Catalyst and its Application for Biodiesel Production by Transesterification. Catalysis Letters, 2009, 131, 574-578.	2.6	50
76	Eggshellâ€Inspired Biomineralization Generates Vaccines that Do Not Require Refrigeration. Angewandte Chemie - International Edition, 2012, 51, 10576-10579.	13.8	50
77	Clean Synthesis of an Economical 3D Nanochain Network of PdCu Alloy with Enhanced Electrocatalytic Performance towards Ethanol Oxidation. Chemistry - A European Journal, 2015, 21, 17779-17785.	3.3	50
78	Platinum Dendritic-Flowers Prepared by Tellurium Nanowires Exhibit High Electrocatalytic Activity for Glycerol Oxidation. ACS Applied Materials & amp; Interfaces, 2015, 7, 17725-17730.	8.0	50
79	Quantum dots decorated gold nanorod as fluorescent-plasmonic dual-modal contrasts agent for cancer imaging. Biosensors and Bioelectronics, 2015, 74, 16-23.	10.1	50
80	Stretch–Stowage–Growth Strategy to Fabricate Tunable Triply-Amplified Electrochemiluminescence Immunosensor for Ultrasensitive Detection of Pseudorabies Virus Antibody. Analytical Chemistry, 2014, 86, 5749-5757.	6.5	49
81	Turn-on near-infrared electrochemiluminescence sensing of thrombin based on resonance energy transfer between CdTe/CdS core small /shell thick quantum dots and gold nanorods. Biosensors and Bioelectronics, 2016, 82, 26-31.	10.1	49
82	Novel impacts of functionalized multi-walled carbon nanotubes in plants: promotion of nodulation and nitrogenase activity in the rhizobium-legume system. Nanoscale, 2017, 9, 9921-9937.	5.6	49
83	A practicable detection system for genetically modified rice by SERS-barcoded nanosensors. Biosensors and Bioelectronics, 2012, 34, 118-124.	10.1	48
84	Regulating the oxidation degree of nickel foam: a smart strategy to controllably synthesize active Ni <sub>3</sub> S <sub>2</sub> nanorod/nanowire arrays for high-performance supercapacitors. Journal of Materials Chemistry A, 2016, 4, 8029-8040.	10.3	48
85	Pt nanozyme for O <sub>2</sub> self-sufficient, tumor-specific oxidative damage and drug resistance reversal. Nanoscale Horizons, 2019, 4, 1124-1131.	8.0	48
86	Precise Chemodynamic Therapy of Cancer by Trifunctional Bacterium-Based Nanozymes. ACS Nano, 2021, 15, 19321-19333.	14.6	47
87	Vaccine Engineering with Dualâ€Functional Mineral Shell: A Promising Strategy to Overcome Preexisting Immunity. Advanced Materials, 2016, 28, 694-700.	21.0	46
88	Highly sensitive enzyme-free immunosorbent assay for porcine circovirus type 2 antibody using Au-Pt/SiO 2 nanocomposites as labels. Biosensors and Bioelectronics, 2016, 82, 177-184.	10.1	45
89	Tumor-triggered transformation of chimeric peptide for dual-stage-amplified magnetic resonance imaging and precise photodynamic therapy. Biomaterials, 2018, 182, 269-278.	11.4	45
90	Au Hollow Nanorods-Chimeric Peptide Nanocarrier for NIR-II Photothermal Therapy and Real-time Apoptosis Imaging for Tumor Theranostics. Theranostics, 2019, 9, 4971-4981.	10.0	44

#	Article	IF	CITATIONS
91	Gastric Acid Powered Nanomotors Release Antibiotics for In Vivo Treatment of <i>Helicobacter pylori</i> Infection. Small, 2021, 17, e2006877.	10.0	44
92	In Situ Nanozymeâ€Amplified NIRâ€II Phototheranostics for Tumorâ€5pecific Imaging and Therapy. Advanced Functional Materials, 2021, 31, 2103765.	14.9	44
93	Novel Porphyrin Zr Metal–Organic Framework (PCN-224)-Based Ultrastable Electrochemiluminescence System for PEDV Sensing. Analytical Chemistry, 2021, 93, 2090-2096.	6.5	43
94	Kanamycin Adsorption on Gold Nanoparticles Dominates Its Label-Free Colorimetric Sensing with Its Aptamer. Langmuir, 2020, 36, 11490-11498.	3.5	42
95	A novel method for methimazole determination using CdSe quantum dots as fluorescence probes. Mikrochimica Acta, 2009, 165, 195-201.	5.0	41
96	Ultrasmall Peptide-Coated Platinum Nanoparticles for Precise NIR-II Photothermal Therapy by Mitochondrial Targeting. ACS Applied Materials & Interfaces, 2020, 12, 39434-39443.	8.0	40
97	Excellent electrochemical performance of nitrogen-enriched hierarchical porous carbon electrodes prepared using nano-CaCO3 as template. Journal of Solid State Electrochemistry, 2013, 17, 2651-2660.	2.5	38
98	pHâ€Responsive Nanoscale Coordination Polymer for Efficient Drug Delivery and Realâ€Time Release Monitoring. Advanced Healthcare Materials, 2017, 6, 1700470.	7.6	36
99	Chemiluminescence Determination of Tetracyclines Using a Tris(2,2'-bipyridine)ruthenium(II) and Potassium Permanganate System Analytical Sciences, 1999, 15, 467-470.	1.6	34
100	Direct electrochemiluminescence of CdTe quantum dots based on room temperature ionic liquid film and high sensitivity sensing of gossypol. Electrochimica Acta, 2010, 55, 1265-1271.	5.2	34
101	Cathodic electrochemiluminescence from self-designed near-infrared-emitting CdTe/CdS/ZnS quantum dots on bare Au electrode. Electrochemistry Communications, 2011, 13, 359-362.	4.7	34
102	Gas–liquid countercurrent integration process for continuous biodiesel production using a microporous solid base KF/CaO as catalyst. Bioresource Technology, 2012, 123, 413-418.	9.6	34
103	Ru(bpy)32+-Silica@Poly-L-lysine-Au as labels for electrochemiluminescence lysozyme aptasensor based on 3D graphene. Biosensors and Bioelectronics, 2018, 106, 50-56.	10.1	34
104	Study on the interaction between CdSe quantum dots and hemoglobin. Spectrochimica Acta - Part A: Molecular and Biomolecular Spectroscopy, 2008, 69, 830-834.	3.9	33
105	Target triggered self-assembly of Au nanoparticles for amplified detection of Bacillus thuringiensis transgenic sequence using SERS. Biosensors and Bioelectronics, 2014, 62, 196-200.	10.1	33
106	Ultrasensitive electrochemical detection of Bacillus thuringiensis transgenic sequence based on in situ Ag nanoparticles aggregates induced by biotin–streptavidin system. Biosensors and Bioelectronics, 2011, 28, 464-468.	10.1	32
107	Versatile Electrochemiluminescence Assays for PEDV Antibody Based on Rolling Circle Amplification and Ru-DNA Nanotags. Analytical Chemistry, 2018, 90, 7415-7421.	6.5	32
108	Pomegranate-Inspired Silica Nanotags Enable Sensitive Dual-Modal Detection of Rabies Virus Nucleoprotein. Analytical Chemistry, 2020, 92, 8802-8809.	6.5	32

#	Article	IF	CITATIONS
109	Dual-Mode Immunosensor for Electrochemiluminescence Resonance Energy Transfer and Electrochemical Detection of Rabies Virus Glycoprotein Based on Ru(bpy) <sub>3</sub> <sup>2+</sup> -Loaded Dendritic Mesoporous Silica Nanoparticles. Analytical Chemistry, 2022, 94, 7655-7664.	6.5	32
110	Solid-state voltammetry-based electrochemical immunosensor for Escherichia coli using graphene oxide–Ag nanoparticle composites as labels. Analyst, The, 2013, 138, 3388.	3.5	31
111	A brilliant sandwich type fluorescent nanostructure incorporating a compact quantum dot layer and versatile silica substrates. Chemical Communications, 2014, 50, 2896.	4.1	31
112	Controlled Synthesis of Au-Island-Covered Pd Nanotubes with Abundant Heterojunction Interfaces for Enhanced Electrooxidation of Alcohol. ACS Applied Materials & amp; Interfaces, 2016, 8, 12792-12797.	8.0	30
113	Intracellular Ca2+ Cascade Guided by NIR-II Photothermal Switch for Specific Tumor Therapy. IScience, 2020, 23, 101049.	4.1	30
114	Gold(iii) enhanced chemiluminescence immunoassay for detection of antibody against ApxIV of Actinobacillus pleuropneumoniae. Analyst, The, 2008, 133, 768.	3.5	29
115	One-step synthesis of water-soluble ZnSe quantum dots via microwave irradiation. Materials Letters, 2010, 64, 1099-1101.	2.6	29
116	An ultrasensitive method for the detection of gene fragment from transgenics using label-free gold nanoparticle probe and dynamic light scattering. Analytica Chimica Acta, 2011, 696, 1-5.	5.4	29
117	Spiny-porous platinum nanotubes with enhanced electrocatalytic activity for methanol oxidation. Journal of Materials Chemistry A, 2015, 3, 1388-1391.	10.3	29
118	Fabrication of Bis-Quaternary Ammonium Salt as an Efficient Bactericidal Weapon Against <i>Escherichia coli</i> and <i>Staphylococcus aureus</i> . ACS Omega, 2018, 3, 14517-14525.	3.5	29
119	A sensitive label-free FRET probe for glutathione based on CdSe/ZnS quantum dots and MnO <sub>2</sub> nanosheets. Analytical Methods, 2018, 10, 4170-4177.	2.7	29
120	Disruption of dual homeostasis by a metal-organic framework nanoreactor for ferroptosis-based immunotherapy of tumor. Biomaterials, 2022, 284, 121502.	11.4	29
121	Ammonia Mediated One-Step Synthesis of Three-Dimensional Porous Pt <sub><i>x</i></sub> Cu <sub>100–<i>x</i></sub> Nanochain Networks with Enhanced Electrocatalytic Activity toward Polyhydric Alcohol Oxidation. ACS Sustainable Chemistry and Engineering, 2017, 5, 11086-11095.	6.7	28
122	Synthesis of biodiesel from rapeseed oil using K2O/γ-Al2O3 as nano-solid-base catalyst. Wuhan University Journal of Natural Sciences, 2009, 14, 75-79.	0.4	27
123	Recent advances in the use of near-infrared quantum dots as optical probes for bioanalytical, imaging and solar cell application. Mikrochimica Acta, 2014, 181, 1485-1495.	5.0	27
124	Acidity-Triggered Tumor Retention/Internalization of Chimeric Peptide for Enhanced Photodynamic Therapy and Real-Time Monitoring of Therapeutic Effects. ACS Applied Materials & Interfaces, 2017, 9, 16043-16053.	8.0	27
125	Aptamer and RVG functionalized gold nanorods for targeted photothermal therapy of neurotropic virus infection in the mouse brain. Chemical Engineering Journal, 2021, 411, 128557.	12.7	27
126	NIR-activated multi-hit therapeutic Ag2S quantum dot-based hydrogel for healing of bacteria-infected wounds. Acta Biomaterialia, 2022, 145, 88-105.	8.3	27

HEYOU HAN

#	Article	IF	CITATIONS
127	Activation of TRPV1 by capsaicin-loaded CaCO3 nanoparticle for tumor-specific therapy. Biomaterials, 2022, 284, 121520.	11.4	27
128	Microwave-assisted synthesis of high-quality CdTe/CdS@ZnS–SiO2 near-infrared-emitting quantum dots and their applications in Hg2+ sensing and imaging. Sensors and Actuators B: Chemical, 2015, 207, 74-82.	7.8	26
129	Electrochemical determination of thiols at single-wall carbon nanotubes and PQQ modified electrodes. Frontiers in Bioscience - Landmark, 2005, 10, 931.	3.0	26
130	Synthesis of p-aminothiophenol-embedded gold/silver core-shell nanostructures as novel SERS tags for biosensing applications. Mikrochimica Acta, 2011, 173, 149-156.	5.0	25
131	Study on the interaction between histidine-capped Au nanoclusters and bovine serum albumin with spectroscopic techniques. Spectrochimica Acta - Part A: Molecular and Biomolecular Spectroscopy, 2014, 118, 897-902.	3.9	25
132	Probing the interactions of CdTe quantum dots with pseudorabies virus. Scientific Reports, 2015, 5, 16403.	3.3	25
133	A direct chemiluminescence method for the determination of nucleic acids using Ru(phen) 3 2+ -Ce(IV) system. Fresenius' Journal of Analytical Chemistry, 1999, 364, 782-785.	1.5	24
134	Chemiluminescence Method for the Determination of Glutathione in Human Serum Using the Ru(phen)3 2+ – KMnO4 System. Mikrochimica Acta, 2006, 155, 431-434.	5.0	24
135	Determination of cypromazine and its metabolite melamine in milk by cationâ€selective exhaustive injection and sweepingâ€capillary micellar electrokinetic chromatography. Journal of Separation Science, 2011, 34, 323-330.	2.5	24
136	Reasonably retard O2 consumption through a photoactivity conversion nanocomposite for oxygenated photodynamic therapy. Biomaterials, 2019, 218, 119312.	11.4	24
137	Bacteria Inspired Internal Standard SERS Substrate for Quantitative Detection. ACS Applied Bio Materials, 2021, 4, 2009-2019.	4.6	24
138	A novel method for sensing of methimazole using gold nanoparticle atalyzed chemiluminescent reaction. Luminescence, 2011, 26, 196-201.	2.9	23
139	Hydrogen-bonding recognition-induced aggregation of gold nanoparticles for the determination of the migration of melamine monomers using dynamic light scattering. Analytica Chimica Acta, 2014, 845, 92-97.	5.4	23
140	Enhanced immunoassay for porcine circovirus type 2 antibody using enzyme-loaded and quantum dots-embedded shell–core silica nanospheres based on enzyme-linked immunosorbent assay. Analytica Chimica Acta, 2015, 887, 192-200.	5.4	23
141	Direct reduction of HAuCl4 for the visual detection of intracellular hydrogen peroxide based on Au-Pt/SiO2 nanospheres. Sensors and Actuators B: Chemical, 2017, 248, 367-373.	7.8	23
142	A cyclic catalysis enhanced electrochemiluminescence aptasensor based 3D graphene/photocatalysts Cu2O-MWCNTs. Electrochimica Acta, 2018, 282, 672-679.	5.2	23
143	Cellular hnRNP A1 Interacts with Nucleocapsid Protein of Porcine Epidemic Diarrhea Virus and Impairs Viral Replication. Viruses, 2018, 10, 127.	3.3	23
144	Near–infrared electrochemiluminesence biosensor for high sensitive detection of porcine reproductive and respiratory syndrome virus based on cyclodextrin-grafted porous Au/PtAu nanotube. Sensors and Actuators B: Chemical, 2017, 240, 586-594.	7.8	22

#	Article	IF	CITATIONS
145	Ratiometric fluorescence sensor for the sensitive detection of Bacillus thuringiensis transgenic sequence based on silica coated supermagnetic nanoparticles and quantum dots. Sensors and Actuators B: Chemical, 2018, 254, 206-213.	7.8	22
146	Determination of DNA by Use of the Molecular "Light Switch" Complex of Ru(bipy) 2 (dppz) 2+. Mikrochimica Acta, 2000, 134, 57-62.	5.0	21
147	Streptococcus suis II immunoassay based on thorny gold nanoparticles and surface enhanced Raman scattering. Analyst, The, 2012, 137, 1259.	3.5	21
148	Mineralized State of the Avian Influenza Virus in the Environment. Angewandte Chemie - International Edition, 2017, 56, 12908-12912.	13.8	21
149	Silica-based nanoenzymes for rapid and ultrasensitive detection of mercury ions. Sensors and Actuators B: Chemical, 2021, 330, 129304.	7.8	21
150	Wavelength Dependence of Fluorescence Quenching of CdTe Quantum Dots by Gold Nanoclusters. Journal of Physical Chemistry C, 2013, 117, 3011-3018.	3.1	20
151	Catalytic hairpin assembly-assisted lateral flow assay for visual determination of microRNA-21 using gold nanoparticles. Mikrochimica Acta, 2019, 186, 661.	5.0	20
152	A portable SERS reader coupled with catalytic hairpin assembly for sensitive microRNA-21 lateral flow sensing. Analyst, The, 2021, 146, 848-854.	3.5	20
153	The behaviors of metal ions in the CdTe quantum dots–H <sub>2</sub> O <sub>2</sub> chemiluminescence reaction and its sensing application. Luminescence, 2009, 24, 271-275.	2.9	19
154	Folic Acid-Targeted and Cell Penetrating Peptide-Mediated Theranostic Nanoplatform for High-Efficiency Tri-Modal Imaging-Guided Synergistic Anticancer Phototherapy. Journal of Biomedical Nanotechnology, 2016, 12, 878-893.	1.1	19
155	Nickel-Ion-Oriented Fabrication of Spiny PtCu Alloy Octahedral Nanoframes with Enhanced Electrocatalytic Performance. ACS Applied Energy Materials, 2019, 2, 2862-2869.	5.1	19
156	Binding induced isothermal amplification reaction to activate CRISPR/Cas12a for amplified electrochemiluminescence detection of rabies viral RNA via DNA nanotweezer structure switching. Biosensors and Bioelectronics, 2022, 204, 114078.	10.1	19
157	Organosilane micellization for direct encapsulation of hydrophobic quantum dots into silica beads with highly preserved fluorescence. Chemical Communications, 2012, 48, 6145.	4.1	18
158	Cobalt ferrite nanozyme for efficient symbiotic nitrogen fixation via regulating reactive oxygen metabolism. Environmental Science: Nano, 2021, 8, 188-203.	4.3	18
159	Tea Polyphenol Liposomes Overcome Gastric Mucus to Treat Helicobacter Pylori Infection and Enhance the Intestinal Microenvironment. ACS Applied Materials & Interfaces, 2022, 14, 13001-13012.	8.0	18
160	Synthesis of multi-branched gold nanoparticles by reduction of tetrachloroauric acid with Tris base, and their application to SERS and cellular imaging. Mikrochimica Acta, 2011, 175, 55-61.	5.0	17
161	A SERS-based immunoassay for porcine circovirus type 2 using multi-branched gold nanoparticles. Mikrochimica Acta, 2013, 180, 1501-1507.	5.0	17
162	Facile synthesis of Cu–In–Zn–S alloyed nanocrystals with temperature-dependent photoluminescence spectra. Materials Letters, 2014, 119, 100-103.	2.6	17

#	Article	IF	CITATIONS
163	A Chimeric Peptide Logic Gate for Orthogonal Stimuliâ€Triggered Precise Tumor Therapy. Advanced Functional Materials, 2018, 28, 1804609.	14.9	17
164	Quantum dots-gold(iii)-based indirect fluorescence immunoassay for high-throughput screening of APP. Chemical Communications, 2009, , 2559.	4.1	16
165	Ultrasensitive detection of porcine circovirus type 2 using gold(iii) enhanced chemiluminescence immunoassay. Analyst, The, 2010, 135, 1680.	3.5	16
166	Toxicity of Molybdenum-Based Nanomaterials on the Soybean–Rhizobia Symbiotic System: Implications for Nutrition. ACS Applied Nano Materials, 2020, 3, 5773-5782.	5.0	16
167	An intelligent platform based on acidity-triggered aggregation of gold nanoparticles for precise photothermal ablation of focal bacterial infection. Chemical Engineering Journal, 2021, 407, 127076.	12.7	16
168	A novel method for the analysis of calf thymus DNA based on CdTe quantum dots-Ru(bpy) 3 2+ photoinduced electron transfer system. Mikrochimica Acta, 2010, 168, 341-345.	5.0	15
169	Investigation the interaction between protamine sulfate and CdTe quantum dots with spectroscopic techniques. RSC Advances, 2016, 6, 10215-10220.	3.6	15
170	One-step synthesis of high-quality homogenous Te/Se alloy nanorods with various morphologies. CrystEngComm, 2015, 17, 3243-3250.	2.6	14
171	Robust Synthesis of Size-Dispersal Triangular Silver Nanoprisms via Chemical Reduction Route and Their Cytotoxicity. Nanomaterials, 2019, 9, 674.	4.1	14
172	Biomimetic Mineralization-Based CRISPR/Cas9 Ribonucleoprotein Nanoparticles for Gene Editing. ACS Applied Materials & Interfaces, 2019, 11, 47762-47770.	8.0	14
173	Electrogenerated chemiluminescence of CdSe quantum dots dispersed in aqueous solution. Frontiers in Bioscience - Landmark, 2007, 12, 2352.	3.0	14
174	DNA Nanotweezers for Biosensing Applications: Recent Advances and Future Prospects. ACS Sensors, 2022, 7, 3-20.	7.8	14
175	The "kinetic capture―of an acylium ion from live aluminum chloride promoted Friedel–Crafts acylation reactions. Organic and Biomolecular Chemistry, 2013, 11, 1810.	2.8	13
176	Universal chitosan-assisted synthesis of Ag-including heterostructured nanocrystals for label-free in situ SERS monitoring. Nanoscale, 2015, 7, 18878-18882.	5.6	13
177	Ultrasensitive evaluation of Ribonuclease H activity using a DNAzyme-powered on-particle DNA walker. Sensors and Actuators B: Chemical, 2020, 304, 127380.	7.8	13
178	Pulse injection analysis with chemiluminescence detection: determination of cinnamic acid using the Ru(bipy)32+-KMnO4 system. Analytica Chimica Acta, 1999, 402, 113-118.	5.4	12
179	Interactions between Water-soluble CdSe Quantum Dots and Gold Nanoparticles Studied by UV-Visible Absorption Spectroscopy. Analytical Sciences, 2007, 23, 651-654.	1.6	12
180	Study on the interaction between 2â€mercaptoethanol, dimercaprol and CdSe quantum dots. Luminescence, 2008, 23, 321-326.	2.9	12

HEYOU HAN

#	Article	IF	CITATIONS
181	Electrochemical sensors based on carbon nanotubes. , 2008, , 459-VIII.		12
182	Synthesis and spectroscopic characterization of water-soluble Mn-doped ZnOxS1â^'x quantum dots. Spectrochimica Acta - Part A: Molecular and Biomolecular Spectroscopy, 2011, 83, 348-352.	3.9	12
183	Facile Synthesis of Quasiâ€Oneâ€Dimensional Au/PtAu Heterojunction Nanotubes and Their Application as Catalysts in an Oxygenâ€Reduction Reaction. Chemistry - A European Journal, 2015, 21, 7556-7561.	3.3	12
184	A Novel Ratiometric Probe Based on Nitrogen-Doped Carbon Dots and Rhodamine B Isothiocyanate for Detection of Fe <sup>3+</sup> in Aqueous Solution. Journal of Analytical Methods in Chemistry, 2016, 2016, 1-7.	1.6	12
185	Intracellular delivery of biomineralized monoclonal antibodies to combat viral infection. Chemical Communications, 2016, 52, 1879-1882.	4.1	12
186	Steric shielding protected and acidity-activated pop-up of ligand for tumor enhanced photodynamic therapy. Journal of Controlled Release, 2018, 279, 198-207.	9.9	12
187	Amorphous nickel boride membrane coated PdCuCo dendrites as high-efficiency catalyst for oxygen reduction and methanol oxidation reaction. Materials Today Energy, 2019, 12, 179-185.	4.7	12
188	Self-assembly of Pt-based truncated octahedral crystals into metal-frameworks towards enhanced electrocatalytic activity. Journal of Materials Chemistry A, 2016, 4, 15169-15180.	10.3	11
189	Graphene Oxide as a Stabilizer for "Clean―Synthesis of High-Performance Pd-Based Nanotubes Electrocatalysts. ACS Sustainable Chemistry and Engineering, 2017, 5, 5191-5199.	6.7	11
190	Assembling PVP-Au NPs as portable chip for sensitive detection of cyanide with surface-enhanced Raman spectroscopy. Analytical and Bioanalytical Chemistry, 2020, 412, 2863-2871.	3.7	11
191	A novel signal amplified electrochemiluminescence biosensor based on MIL-53(Al)@CdS QDs and SiO2@AuNPs for trichlorfon detection. Analyst, The, 2021, 146, 1295-1302.	3.5	11
192	Facile synthesis and characterization of CdTe quantum dots–polystyrene fluorescent composite nanospheres. Materials Letters, 2009, 63, 2224-2226.	2.6	9
193	Near-infrared electrogenerated chemiluminescence from quantum dots. Reviews in Analytical Chemistry, 2013, 32, .	3.2	9
194	Synthesis of Tellurium Fusiform Nanoarchitectures by Controlled Living Nanowire Modification. Journal of Physical Chemistry C, 2016, 120, 12305-12312.	3.1	9
195	Pd@Pt Core–Shell Nanodots Arrays for Efficient Electrocatalytic Oxygen Reduction. ACS Applied Nano Materials, 2019, 2, 3695-3700.	5.0	9
196	Synthesis and Spectroscopic Characterization of Water-Soluble Fluorescent Ag Nanoclusters. Journal of Analytical Methods in Chemistry, 2013, 2013, 1-5.	1.6	8
197	An aqueous platinum nanotube based fluorescent immuno-assay for porcine reproductive and respiratory syndrome virus detection. Talanta, 2015, 144, 324-328.	5.5	7
198	Van-mediated self-aggregating photothermal agents combined with multifunctional magnetic nickel oxide nanoparticles for precise elimination of bacterial infections. Journal of Nanobiotechnology, 2022, 20, .	9.1	7

#	Article	IF	CITATIONS
199	Perturbation of the tris(2,2′â€bipyridine) ruthenium(II)â€catalyzed Belousov–Zhabotinsky oscillating chemiluminescence reaction by <scp>l</scp> â€cysteine and its application. Luminescence, 2009, 24, 300-305.	2.9	6
200	Sensitive immunoassay for porcine pseudorabies antibody based on fluorescence signal amplification induced by cation exchange in CdSe nanocrystals. Mikrochimica Acta, 2013, 180, 303-310.	5.0	6
201	Intravital imaging of Bacillus thuringiensis Cry1A toxin binding sites in the midgut of silkworm. Analytical Biochemistry, 2014, 447, 90-97.	2.4	6
202	Evaluation of Biological Toxicity of CdTe Quantum Dots with Different Coating Reagents according to Protein Expression of Engineering <i>Escherichia coli</i> . Journal of Nanomaterials, 2015, 2015, 1-7.	2.7	6
203	Nitrogen-doped graphene quantum dots doped silica nanoparticles as enhancers for electrochemiluminescence thrombin aptasensors based on 3D graphene. Journal of Solid State Electrochemistry, 2019, 23, 2579-2588.	2.5	6
204	A New Type of Capping Agent in Nanoscience: Metal Cations. Small, 2019, 15, 1900444.	10.0	6
205	Biogenic Hybrid Nanosheets Activated Photothermal Therapy and Promoted Anti-PD-L1 Efficacy for Synergetic Antitumor Strategy. ACS Applied Materials & Interfaces, 2020, 12, 29122-29132.	8.0	6
206	Sequential assembled chimeric peptide for precise synergistic phototherapy and photoacoustic imaging of tumor apoptosis. Chemical Engineering Journal, 2022, 427, 130775.	12.7	6
207	Chemiluminescence Determination of Gluconic Acid in Pharmaceutical Formulations using Ru(bipy) <sub>3</sub> <sup>2+</sup> – KIO <sub>4</sub> – Ce(IV) System. Analytical Letters, 1999, 32, 2297-2310.	1.8	5
208	Platinum-based nitrogen-doped porous C x N 1-x compounds used as a transducer for sensitive detection of hydrogen peroxide. Electrochimica Acta, 2016, 209, 661-670.	5.2	5
209	Pd–Au heterostructured nanonecklaces with adjustable interval and size as a superior catalyst for degradation of 4-nitrophenol. CrystEngComm, 2017, 19, 5686-5691.	2.6	5
210	Multifunctional Nanosystems with Enhanced Cellular Uptake for Tumor Therapy. Advanced Healthcare Materials, 2022, 11, e2101703.	7.6	5
211	Novel approach to enhance Bradyrhizobium diazoefficiens nodulation through continuous induction of ROS by manganese ferrite nanomaterials in soybean. Journal of Nanobiotechnology, 2022, 20, 168.	9.1	5
212	Development of a Direct Chemiluminescence Method for the Determination of Nucleic Acids Based upon Their Reaction with Cerium(IV) in the Presence of Rutheniumtrisdipyridine Analytical Sciences, 1999, 15, 885-888.	1.6	4
213	A Simple and Efficient Method for Synthesizing Te Nanowires from CdTe Nanoparticles with EDTA as Shape Controller under Hydrothermal Condition. Journal of Nanomaterials, 2012, 2012, 1-7.	2.7	4
214	Facile Synthesis and Characterization of Au Nanoclusters-Silica Fluorescent Composite Nanospheres. Journal of Nanomaterials, 2013, 2013, 1-5.	2.7	4
215	Two-dimensional colloidal crystal assisted formation of conductive porous gold films with flexible structural controllability. Journal of Colloid and Interface Science, 2015, 437, 291-296.	9.4	4
216	Timeâ€resolved fluorescent microsphere lateral flow biosensors for rapid detection of <i>Candidatus</i> Liberibacter asiaticus. Plant Biotechnology Journal, 2022, 20, 1235-1237.	8.3	4

#	Article	IF	CITATIONS
217	Theoretical Analysis of T-lymphocytes Electroporation Model. , 2008, , .		2
218	Mineralized State of the Avian Influenza Virus in the Environment. Angewandte Chemie, 2017, 129, 13088-13092.	2.0	2
219	Innentitelbild: Mineralized State of the Avian Influenza Virus in the Environment (Angew. Chem.) Tj ETQq1 1 0.784	4314 rgBT 2.0	/8verlock 1
220	Light-Induced Caspase-3-Responsive Chimeric Peptide for Effective PDT/Chemo Combination Therapy with Good Compatibility. ACS Applied Bio Materials, 2020, 3, 2392-2400.	4.6	0
221	Effect of TransferredAnsferred Submount Materials on Properties of GaN-Based LED Chips Grown on Si Substrate. Guangxue Xuebao/Acta Optica Sinica, 2008, 28, 143-145.	1.2	0